



# Lactoferrin alleviates Western diet-induced cognitive impairment through the microbiome-gut-brain axis

Qian He<sup>a</sup>, Li-Li Zhang<sup>a</sup>, Deming Li<sup>a</sup>, Jiangxue Wu<sup>a</sup>, Ya-Xin Guo<sup>a</sup>, Jingbo Fan<sup>a,b</sup>,  
Qingyang Wu<sup>c</sup>, Hai-Peng Wang<sup>d,e</sup>, Zhongxiao Wan<sup>a</sup>, Jia-Ying Xu<sup>d</sup>, Li-Qiang Qin<sup>a,\*</sup>

<sup>a</sup> Department of Nutrition and Food Hygiene, School of Public Health, Soochow University, 199 Ren'ai Road, Suzhou, Jiangsu, 215123, China

<sup>b</sup> Laboratory Center, Medical College of Soochow University, 199 Ren'ai Road, Suzhou, Jiangsu, 215123, China

<sup>c</sup> School of Life Science, Chinese University of Hong Kong, 7th Floor, Yasumoto International Academic Park, 999077, China

<sup>d</sup> State Key Laboratory of Radiation Medicine and Protection, School of Radiation Medicine and Protection, Soochow University, 199 Ren'ai Road, Suzhou, Jiangsu, 215123, China

<sup>e</sup> Department of Cardiovascular, The First Affiliated Hospital of Soochow University, 188 Shizi Street, Suzhou, Jiangsu, 215006, China

## ARTICLE INFO

Handling Editor: Professor A.G. Marangoni

### Keywords:

Lactoferrin

'Western'-style diets

Neuroinflammation

Cognitive impairment

Behavioral change

Hippocampus

Gut microbiota

Microbiome-gut-brain axis

## ABSTRACT

Lactoferrin (Lf) has been shown to benefit cognitive function in several animal models. To elucidate the underlying mechanisms, male C57BL/6J mice were randomly divided into the control (CON), Western-style diets (WD), lactoferrin (Lf), and Lf + antibiotics (AB) groups. The Lf group was intragastrically administered with Lf, and the Lf + AB group additionally drank a solution with antibiotics. After 16 weeks of intervention, Lf improved the cognitive function as indicated by behavioral tests. Lf also increased the length and curvature of postsynaptic density and upregulated the related protein expression, suggesting improved hippocampal neurons and synapses. Lf suppressed microglia activation and proliferation as revealed by immunofluorescence analysis. Lf decreased the serum levels of pro-inflammatory cytokines and downregulated their protein expressions in the hippocampus region. Lf also inhibited the activation of NF- $\kappa$ B/NLRP3 inflammasomes in the hippocampus. Meanwhile, Lf upregulated the expression of tight junction proteins, and increased the abundance of Bacteroidetes at phylum and *Roseburia* at genus, which are beneficial for gut barrier and cognitive function. The antibiotics eliminated the effects of long-term Lf intervention on cognitive impairment in the Lf + AB group, suggesting that gut microbiota participated in Lf action. Short-term Lf intervention (2 weeks) prevented WD-induced gut microbiota alteration without inducing behavioral changes, supporting the timing sequence of gut microbiota to the brain. Thus, Lf intervention alleviated cognitive impairment by inhibiting microglial activation and neuroinflammation through the microbiome-gut-brain axis.

## 1. Introduction

High-energy-dense Western-style diets (WD) rich in fat and simple carbohydrates contribute to the development of obesity and obesity-related chronic diseases (Fan et al., 2017). Obesity is a risk factor for neurodegenerative diseases, such as Alzheimer's disease (AD) and Parkinson's disease (PD) (Leigh and Morris, 2020). Chronic inflammation is one of the mechanisms contributing to the development of obesity-related diseases, including neurodegenerative diseases. Microglia are the resident immune cells of the brain, and their activation induces the secretion of pro-inflammatory factors and hippocampal inflammation (Farruggia and Small, 2019). Neuroinflammation has

been proposed to be an important pathophysiological hallmark underlying these diseases (Kwon and Koh, 2020). Thus, neuroinflammation improvement is an optional way to prevent cognitive impairment.

Stable gut microbiota composition is critical in sustaining the balance of intestinal barrier integrity and inflammation, thus positively regulating brain development and behavior through the microbiome-gut-brain axis (Diaz Heijtz et al., 2011; Buford, 2017). The gut microbiome is strongly associated with neurodegenerative diseases, modulates behavior, and contributes to neurological disorders (Fung et al., 2017). Gut dysbiosis may promote amyloid-beta aggregation, neuroinflammation, and oxidative stress in the pathogenesis of AD (Liu et al., 2020). Transferring the microbiota of AD patients to amyloid precursor

\* Corresponding author.

E-mail address: [qinliqiang@suda.edu.cn](mailto:qinliqiang@suda.edu.cn) (L.-Q. Qin).

<https://doi.org/10.1016/j.crfs.2023.100533>

Received 31 March 2023; Received in revised form 12 June 2023; Accepted 13 June 2023

Available online 15 June 2023

2665-9271/© 2023 Published by Elsevier B.V. This is an open access article under the CC BY-NC-ND license (<http://creativecommons.org/licenses/by-nc-nd/4.0/>).

protein (APP)/presenilin-1 (APP/PS1) mice can promote microglia activation and inflammatory response in the hippocampus, further aggravating the pathological progression of AD and leading to declined cognitive and behavioral abilities (Shen et al., 2020). Therefore, microbial alteration is involved in neuroinflammation and cognitive impairment (Bruce-Keller et al., 2015).

These neurodegenerative diseases are currently not curable; however, the Lancet Commission reported that more than one-third of cases may be prevented by addressing lifestyle factors, including diet (Livingston et al., 2017). Emerging evidence suggests that diets can influence the gut microbiome by modulating brain functions through the gut-brain axis. Lactoferrin (Lf) is a component of whey protein and possesses multiple functions, such as anti-inflammatory, antibacterial, reactive oxygen species (ROS) modulator, antiviral, and antitumor immunity effects (Brimelow et al., 2017). A population-based study found that salivary Lf is associated with cortical amyloid-beta load, cortical integrity, and memory in aging (Reseco et al., 2021). Lf administration could improve the cognitive function of AD patients by affecting key inflammatory and oxidative stress (Mohamed et al., 2019). Lf was detected in senile plaques and neurofibrillary tangles (NFTs) from APP transgenic (APP-Tg) mice and AD patients (Guo et al., 2017; Abdelhamid et al., 2020). Several animal models were used to investigate the effect of Lf administration on cognitive function. Both Lf and hydrolyzed Lf attenuated memory impairment by inhibiting the amyloidogenic processing of APP in APP-Tg mice (Abdelhamid et al., 2020). Similarly, intranasal Lf administration improved cognitive function in APP/PS1 mice (Guo et al., 2017). In addition, the intervention of Lf and other whey proteins was observed to modulate gut microbiota (Boscaini et al., 2019; Hu et al., 2020), which is strongly associated with cognitive impairment (Fung et al., 2017; Liu et al., 2020). However, our previous study found that Lf did not affect cognitive function but benefited gut microbiota homeostasis in young and middle-aged APP/PS1 mice (Zhou et al., 2021). Thus, the relationship between Lf and cognitive impairment remains inconclusive, and the mechanisms underlying this relationship are not fully elucidated.

This study aimed to investigate whether Lf alleviates cognitive impairment through neuroinflammation and gut microbiota in obese mice fed WD for 16 weeks. Cognitive function was measured by behavioral tests. Neurological condition was observed by analyzing the ultrastructure of hippocampal synapses. Neuroinflammation was detected by examining microglial activation and proliferation. Toll-like receptor 4 (TLR4)/nuclear factor kappa-B (NF- $\kappa$ B) signaling and NOD-like receptor thermal protein domain associated protein 3 (NLRP3) inflammasomes in the hippocampus were further analyzed. For the study on the role of gut microbiota, the intestinal microbiota of one group was depleted by administering broad-spectrum antibiotic cocktail. Some of the mice in each group were killed at 2 weeks to analyze whether the gut microbiota is altered prior to behavioral changes and to confirm the microbiome-gut-brain axis.

## 2. Materials and methods

### 2.1. Animals and grouping

Sixty-six male C57BL/6J mice aged 3 months were purchased from Shanghai Jihui Laboratory Animal Care Company (Shanghai, China) and housed in a standard specific pathogen-free animal laboratory (temperature 20–26 °C; relative humidity 40–60%; 12 h light–dark cycle) with access to food and liquid ad libitum. All procedures were performed in accordance with the Guidelines in the Care and Use of Animals and with the approval of the Soochow University Animal Welfare Committee (No. 202009A661). After 1 week of acclimation, the mice were randomly divided into four groups: the CON (n = 18), WD (n = 18), Lf (n = 18), and Lf + antibiotics (AB) (n = 12). The mice in the CON group were fed with a standard diet (AIN93G, kcal%: protein 20.3%, carbohydrate 63.9%, and fat 15.8%), while the other three groups were fed

with WD (D18061501, kcal%: protein 17%, carbohydrate 43%, and fat 40%). Both diets were purchased from Dyets Inc., (Wuxi, Jiangsu, China) (Table A.1). Native bovine Lf (92.5% purity) was obtained from Hilmar Cheese Company (CA, USA). Based on the previous animal study (Abdelhamid et al., 2020), the mice in the Lf group were intragastrically administered with Lf at approximately 500 mg/kg body weight five times a week. To achieve this amount, Lf was prepared as a 65 mg/mL solution in distilled water, and orally administered to mice (25–30 g) in a volume of approximately 0.2 mL. The mice in the Lf + AB group were administered the same dose of Lf and drank the solution containing antibiotics (ampicillin 1 g/L, metronidazole 1 g/L, both from Fujifilm Wako Pure Chemical Corporation, Tokyo, Japan; neomycin 1 g/L, and vancomycin 0.25 g/L, both from Sigma-Aldrich Co. Ltd, MO, USA), as described previously by Shi et al. (2020). Mice drink approximately 3 g of water every day. Thus, they received approximately 0.75 mg of vancomycin and 3 mg of ampicillin, metronidazole, and neomycin. Drinking water was freshly prepared in distilled water every 2 days. Body weight, diet, and water amounts were recorded weekly.

After 2 weeks, a short-term experiment was performed. Six mice from the CON, WD, and Lf groups were randomly selected for the behavior tests. After the behavior tests, the mice were euthanized and their cecal contents were collected for gut microbiota analyses. The remaining mice in the four groups (each group n = 12) were maintained under the same conditions. The experiments were ended at 16 weeks and performed the following analysis. The experimental design and animal groups are shown in Fig. A1.

### 2.2. Behavioral tests

The nesting behavior test, novel object recognition (NOR) test, and Morris water maze (MWM) test were used to examine recognition memory and spontaneous rodent behaviors. The results were recorded by a video tracking system (SuperMaze software, Shanghai Xinruan Information Technology Co., Ltd., China). Using the previous studies (Bevins and Besheer, 2006; Deacon, 2006; Vorhees and Williams, 2006) as references, the tests procedures were briefly described.

**Nesting behavior test:** Approximately 1 h before the dark phase, the mice were transferred to individual testing cages with an unscented paper towel of uniform size. The next morning, the nests were assessed on a rating scale from 1 to 5: 1) paper towels intact; 2) paper towels remain largely intact (>90% complete); 3) paper towels are mostly chopped but no recognizable nest position; 4) a flat nest can be seen and the paper towels are arranged in a certain direction; and 5) the nest is constructed higher than the mouse, and the circumference can completely surround the mouse.

**NOR test:** The mice were habituated to the testing arena with two identical objects for 10 min for 2 consecutive days. On day 3, the mice were first permitted to explore the arena for 10 min for the familiarization phase and then returned to their home cages. After 30 min, one of the objects was replaced with a novel object of similar size, and the mice were placed in the testing arena. Short-term object memory was assessed by object exploration defined as an animal's nose approaching the object inside a 2 cm radius around the objects.

**MWM test:** MWM test was routinely performed using a water maze device with a 150 cm diameter and 35 cm high circular pool (XR-XM101, Shanghai Xinruan Information Technology Co. Ltd., Shanghai, China). The mice were individually housed for 1 day and then acquisitively trained over 5 consecutive days with four trials per day. On day 6, the platform was removed and the mice were returned to the device. Latency to the platform, time spent in the target quadrant, and the number of platform crossings were recorded to indicate the degree of memory consolidation.

### 2.3. Biochemical analyses

At the end of the experiment, the mice were deprived of food for 12 h

and sacrificed. Serum was separated by centrifugation (3000 g, at 4 °C for 15 min) and stored at -80 °C. Serum total cholesterol (TC), triglyceride (TG), low-density lipoprotein cholesterol (LDL-C), and high-density lipoprotein cholesterol (HDL-C) were detected using commercial kits (Applygen Technologies Inc., Beijing, China). Serum TNF- $\alpha$  and IL-6 were analyzed by ELISA kits (MultiSciences (Lianke) Biotech Co., Ltd., Hangzhou, China).

#### 2.4. Hematoxylin-eosin (HE) staining and immunofluorescence double labeling

The mice from the CON, WD, and Lf groups were perfused via the tips of the heart with phosphate-buffered saline (PBS, pH 7.2) and 4% paraformaldehyde. The mouse brains were then maintained in 4% paraformaldehyde for 48 h and embedded into a paraffin block. The paraffin-embedded brains were sagittally cut into 4  $\mu$ m-thick slices. For histopathological examination, the sections including cortex and hippocampus (cornuammonis (CA) and dentate gyrus (DG)) were assessed with routine HE staining. For immunofluorescence double labeling, the sections were blocked with bovine serum albumin and then incubated with a primary antibody mixture including mouse anti-BrdU (1:500, Wuhan Servicebio Technology Co., Ltd., Wuhan, China) and rabbit anti-Ib $\alpha$ 1 (1:500, Servicebio) overnight at 4 °C. After incubation with the secondary antibodies for 1 h at room temperature in the darkness, DAPI (Invitrogen, CA, USA) was applied for counterstaining and images were taken using Panoramic Midi (3D Histech Ltd., Budapest, Hungary).

#### 2.5. Analysis of the synapse ultrastructure in the hippocampus

After undergoing transcardial perfusion with saline, the brain tissues were taken out and a 1 mm<sup>3</sup> tissue block was cut from the hippocampus. After being dehydrated in ascending graded ethanol series and embedded in epoxy resin, the block was fixed in 2% paraformaldehyde-2.5% glutaraldehyde mixture for 24 h and treated post-fixation with 1% osmium tetroxide (OsO<sub>4</sub>) for 2 h. Sections (70 nm) were cut and stained with 4% uranyl acetate and 0.5% lead citrate. Images were observed under a JEM-1230 transmission electron microscope (TEM) equipped with a side inserted BioScan camera (Veleta, EMSIS GmbH, Germany). Synaptic morphometrics (postsynaptic density, synaptic clefts width and the curvature of the synaptic interface) were analyzed by the previously described methods using Image J software (Pan et al., 2021).

#### 2.6. Measurements of colon length and colonic mucus layer thickness

The distal colon was removed quickly, and its length was measured using a high-precision electronic digital caliper (Deli, dl-150, Ningbo, Zhejiang). The colon was cleaned, and some parts of the colon tissues were stored at -80 °C for further use. The remaining descending colons were fixed in Carnoy's solution. After being washed in anhydrous methanol, the tissues were placed in cassettes and stored in anhydrous methanol. To detect colonic mucus layer thickness, the tissues were embedded in paraffin and cut into 5  $\mu$ m-thick slices. After mounting on glass slides with Alcian blue staining, the thickness of the colonic mucus layer was observed under an eclipse microscope (Nikon, Tokyo, Japan).

#### 2.7. Quantitative real-time polymerase chain reaction (qRT-PCR) analysis

Total mRNA was extracted from the tissues using the RNA quick purification kit (Yeasen Biotechnology, Shanghai, China), and cDNA was synthesized using Hifair<sup>®</sup>III 1st Strand cDNA Synthesis SuperMix (Yeasen Biotechnology, Shanghai, China) and GeneAmp PCR system 9700 (Applied Biosystems) following the manufacturer's instructions. qRT-PCR was performed using Hieff<sup>®</sup> qPCR SYBR Green Master Mix (Yeasen Biotechnology, Shanghai, China) and QuantStudio 6 Flex Real-Time PCR System (Thermo, USA). Relative mRNA expression level was

determined using the 2- $\Delta\Delta$ Ct method with GAPDH as the internal reference control (Livak and Schmittgen, 2001). Table A.2 shows the gene-specific mouse primers.

#### 2.8. Western blot analysis

The tissues were homogenized in ice-cold RIPA lysis buffer (Beyotime, Shanghai, China) and supplemented with complete EDTA-free protease inhibitor cocktail and PhosSTOP Phosphatase Inhibitor. The protein samples were mixed with 5  $\times$  dual color protein loading buffer (Fudebio, Hangzhou, China) and boiled at 98 °C for 10 min. Equal amounts of protein (30  $\mu$ g/lane) were loaded on a SDS-PAGE gel at a constant voltage and then transferred to a polyvinylidene difluoride membrane (Millipore, MA, USA). After being blocked and incubated with the primary and secondary antibodies, the bands were visualized using a chemiluminescence image analysis system (Tanon, Shanghai, China) with FDBioFemto ECL (Fudebio, Hangzhou, China). The band intensities were quantified using Gel-Pro Analyzer software (Media Cybernetics, Maryland, USA). The primary antibodies were included the following: synaptosomal associated proteins 25 (SNAP-25; Abcam, ab109105), postsynaptic density proteins 95 (PSD-95; CST, 3450), Ib $\alpha$ 1 (Abcam, ab178846), TNF- $\alpha$  (Abcam, ab215188), IL-6 (Abcam, ab233706), NLRP3 (Abcam, ab263899), IL-18 (Abcam, ab243091), IL-1 $\beta$  (Abcam, ab254360), caspase-1 (Abcam, ab207802), TLR4 (Abcam, ab22048), myeloid differentiation factor 88 (MyD88; Abcam, ab133739), NF- $\kappa$ B p65 (Abcam, ab32536), GAPDH (ABclonal, AC033), ZO-1 (ABclonal, A11417), occludin (ABclonal, A12621) and  $\beta$ -actin (ABclonal, AC026).

#### 2.9. 16S rRNA gene sequencing and analysis

DNA was extracted by a PowerMax extraction kit (MoBio Laboratories, CA, USA) following the product introduction. The V3-V4 region of the bacteria's 16S rRNA gene was amplified using a thermocycler PCR system. PCR products were purified using AMPure XP Beads (Beckman Coulter, IN, USA) and quantified using PicoGreen dsDNA Assay Kit (Invitrogen); Finally, the sequencing was conducted using 2  $\times$  150 bp pair-end configuration on Illumina HiSeq4000 platform. The 16S rRNA data were analyzed using Quantitative Insights into Microbial Ecology (QIIME) and R package (v3.2.0). Quality filtering was performed to obtain the effective sequence, and the effective sequence clustering with a 97% confidence threshold was grouped into operation taxonomic units (OTUs) by Vsearchv2.4.4. Representative sequences of OTUs were selected and annotated based on SILVA128. The community composition of each sample and the abundance of OTUs were counted at the levels of kingdom, phylum, class, order, family, genus, and species. Alpha diversity index (including Chao1, abundance-based coverage estimator (ACE), Shannon and Simpson indexes) was calculated with QIIME software to compare OTUs abundance, evenness, and the difference between groups. Linear discriminant analysis effect size (LefSe) was used to select the biomarkers for comparison among the groups (Bioproject PRJNA 982274).

#### 2.10. Statistical analysis

Data were analyzed using the statistical package SPSS (Version 20, Chicago, USA). Differences among the intervention groups were determined using one-way analysis of variance (ANOVA) followed by least significant difference (LSD, if homogeneity of variance was satisfied) or Tamhane's T2 (if homogeneity of variance was not satisfied) for multiple comparisons. A p-value of <0.05 was considered to be statistically significant. For the results of this study, data were quantified and reported as mean  $\pm$  SEM. For 16S rRNA gene sequencing analysis, all reads were deposited and grouped into OTU at a sequence identity of 97%. The taxonomic affiliation of the OTUs was determined with quantitative insights into microbial ecology (QIIME, version 1.8.0)

against the Greengenes database version 13.8.

### 3. Results

#### 3.1. Lf intervention decreased body weight and improved lipid profiles

During the experimental period, the mice fed with WD had heavier body weights than those fed with a standard diet. However, the body weight was significantly decreased by 28.3% in the Lf group, compared with the WD group (Fig. 1A and B). WD feeding resulted in a significant accumulation of white adipose tissues. A significant decrease in the weight of subcutaneous, perirenal and epididymal fats was observed in the Lf group (Fig. 1C). Although the mice in the WD group had less food intake, there was no significant difference in energy intake among the three groups (Fig. 1D). WD feeding caused dyslipidemia due to increased serum TC, TG, and LDL and decreased serum HDL in the WD group. This phenomenon was reversed in the Lf group (Fig. 1E-H).

#### 3.2. Lf intervention ameliorated cognitive impairment

Nesting behavior was impaired in the WD and improved in the Lf group (Fig. 2A), as quantitatively confirmed by the nesting score (Fig. 2B). In the NOR test, the mice in the WD group had a significantly decreased number of head explorations and exploration time with a novel object. These two indexes were restored by Lf intervention, suggesting the improvement of novel object recognition memory (Fig. 2C-E). The total exploration time of objects was comparable among the three groups (Fig. 2F). In the MWM test, the mice in the WD group spent more time and distance to find the platform from the third day. However, the time and distance significantly reduced in the Lf group compared with the WD group (Fig. 2G-I). Compared with the WD group, Lf significantly decreased escape latency by 30.5% and increased the numbers crossing platform and proportion of distance in the target quadrant by 57.1% and 27.7%, respectively (Fig. 2J-L). During the test, the mice in the 3 groups swim at a similar speed (Fig. 2M). Thus, Lf ameliorated the WD-induced impairment of cognitive function.

#### 3.3. Lf intervention improved the hippocampal neurons and synapses

The hippocampus and cortex are the main regions implicated in

cognitive processing, learning, and memory. HE staining showed that the mice in the CON group had normal morphology of neurons in the hippocampus region. Swollen neurons with a loose structure, increased nuclear pyknosis, and neuronal damages were observed in the WD group; these neuronal pathological changes were partially ameliorated in the Lf group (Fig. 3A). TEM analysis showed that WD feeding reduced the length, width, and curvature of the PSD in the hippocampus region (Fig. 3B). Quantitatively, their length and curvature were significantly increased by 25.5% and 79.1% in the Lf group, compared with the WD group (Fig. 3C-E). Meanwhile, the decreased protein expression levels of PSD-95 and SNAP-25 in the WD group were significantly upregulated in the Lf group (Fig. 3F-H). Thus, Lf improved the WD-induced damage of hippocampal neurons and synapses.

#### 3.4. Lf intervention suppressed microglia activation and inflammation in the brain

The hippocampus and cortex are particularly vulnerable to inflammation (Jeon et al., 2012; Dinel et al., 2014). With Iba1 as the marker of microglial activation in the brain (Lituma et al., 2021), immunofluorescence analysis showed that WD feeding increased the number of activated microglia in the hippocampal regions. However, the number of activated microglia with Iba1<sup>+</sup> was significantly decreased by 16.7% in the Lf group, compared with the WD group (Fig. 4A and B). BrdU is incorporated in the S-phase cells in the cell cycle to detect cell proliferation (Cheng et al., 2019). Double staining further showed significantly more BrdU<sup>+</sup> Iba1<sup>+</sup> positive cells in the WD group than in the CON group, and these positive cells were significantly inhibited by 31.5% in the Lf group (Fig. 4A and C). Meanwhile, WD feeding upregulated the protein expression levels of TNF- $\alpha$  and IL-6 significantly in the cortex and hippocampus, which were significantly inhibited by Lf intervention (Fig. 4F and G). Similarly, compared with those in the CON group, the serum levels of TNF- $\alpha$  and IL-6 significantly increased in the WD group, but were significantly lower in the Lf group than in the WD group (Fig. 4H and I). Thus, Lf prevented WD-induced microglia activation and neuroinflammation.

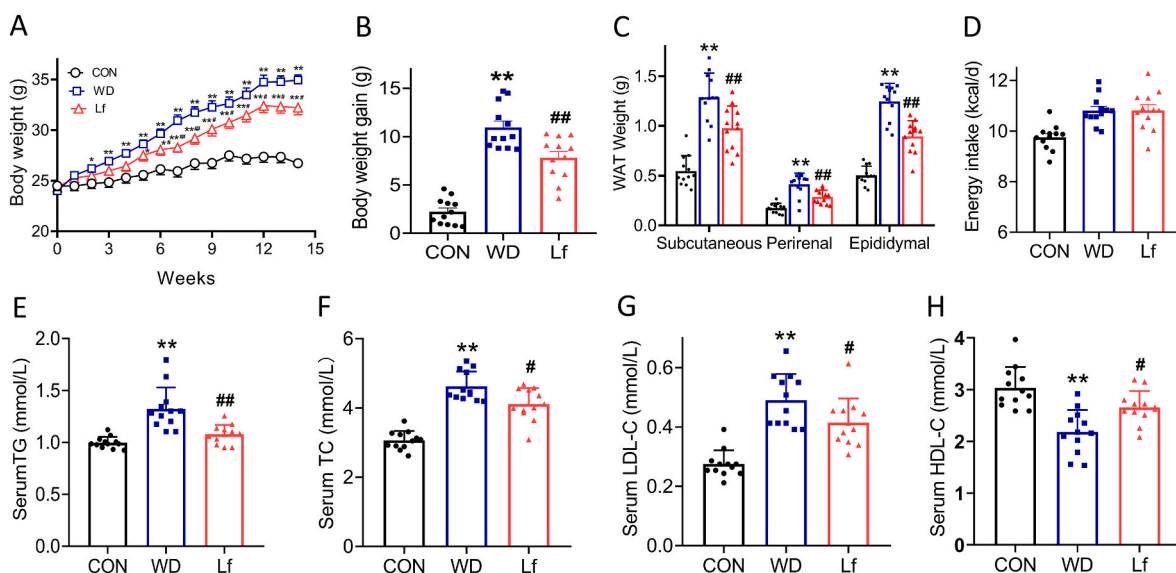


**Fig. 1.** Lf intervention decreased body weight and improved lipid profiles in mice fed with 'Western'-style diets (WD). A. body weight trend during the experiment; B. body weight gain at the end of experiment; C. white adipose tissue (WAT) weight; D. energy intake; E-H. blood lipid profile. E. serum triglyceride (TG); F. serum total cholesterol (TC); G. serum low-density lipoprotein cholesterol (LDL-C); H. serum high-density lipoprotein cholesterol (HDL-C). n = 12 mice each group. \*P < 0.05 vs. the CON group; \*\*\*P < 0.01 vs. the CON group. #P < 0.05 vs., the WD group; ##P < 0.01 vs. the WD group.

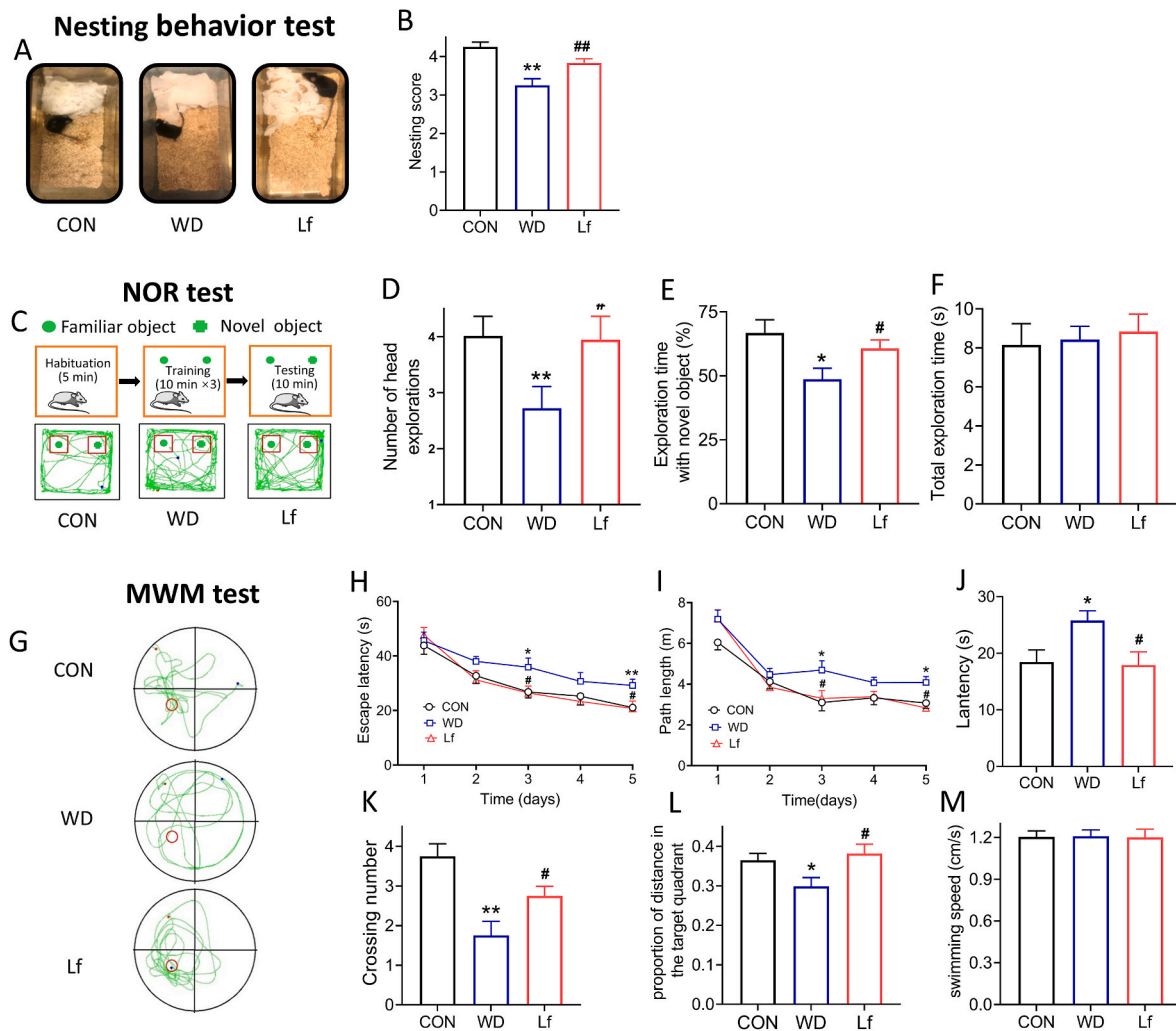


**Fig. 2.** Lf intervention ameliorated ‘Western’-style diets (WD)-induced cognitive impairment in mice. A, and B. nesting behavior test. A. pictures of test; B. the nest scores. C-F. novel object recognition (NOR) test. C. NOR diagram; D. the number of head explorations; E. percentage of time spent with the novel object to total object exploration time; F. the total object exploration time; G-M. Morris water maze (MWM) test. G. trajectory diagram after removing the escape platform; H. escape latency; I. escape path length; J. escape latency after removing the escape platform; K. crossing number; L. proportion of distance in the target quadrant; M. swimming speed. n = 12 mice each group. \*P < 0.05 vs. the CON group; \*\*P < 0.01 vs. the CON group. #P < 0.05 vs., the WD group; ##P < 0.01 vs. the WD group.

### 3.5. Lf intervention inhibited the activation of NF- $\kappa$ B/NLRP3 inflammasomes in the hippocampus

NF- $\kappa$ B/NLRP3 inflammasome signaling pathways in the hippocampus were detected by PCR and Western blot. The results showed that the mRNA and protein expression of NF- $\kappa$ B p65 and MyD88 levels were upregulated in the WD group. NF- $\kappa$ B can be activated by TLR4, which was also upregulated by WD. By contrast, Lf intervention downregulated the mRNA and protein expression of TLR4, MyD88, and NF- $\kappa$ B p65 (Fig. 5A-C). Stimulation of the NF- $\kappa$ B signal transduction pathway is an early event for NLRP3 inflammasome activation (Bauernfeind et al., 2009). The results showed that the mRNA and protein expression of NLRP3, caspase-1, IL-18, and IL-1 $\beta$  were significantly higher in the WD group than in the CON group. Nevertheless, Lf significantly downregulated the expression of these four proteins, and the mRNA of IL-18 and IL-1, compared with those in the WD group (Fig. 5D-F). Therefore, Lf inhibited the WD-induced activation of the NF- $\kappa$ B/NLRP3 inflammasome signaling pathway in the hippocampus.

### 3.6. Lf intervention maintained colonic integrity and alleviated inflammation

The colonic physiological function is dependent on the colon length. At autopsy, the colon of the mice in the WD group was significantly shortened. However, Lf intervention significantly increased the length by 9.1%, and its length is almost the same as the CON group (Fig. 6A and B). Alcian blue staining showed that the mucosal thickness in the colon was decreased in the WD group compared with that in the CON group, and was increased by Lf intervention (Fig. 6C). In terms of the integrity of the gut barrier, the expression of tight junction proteins occludin and ZO-1 was significantly downregulated in the WD group, but upregulated in the Lf group. A significant difference in ZO-1 protein was observed in the Lf group compared with that in the WD group (Fig. 6D and E). Given that shortened colon length and damaged colonic integrity are associated with inflammation, further analysis revealed that Lf intervention significantly inhibited the WD-induced upregulation of protein expression of TNF- $\alpha$ , IL-6, and IL-1 $\beta$  in the colon tissues (Fig. 6F and G). These results indicated that Lf maintained colonic function, which provides the basis for gut microbiota.

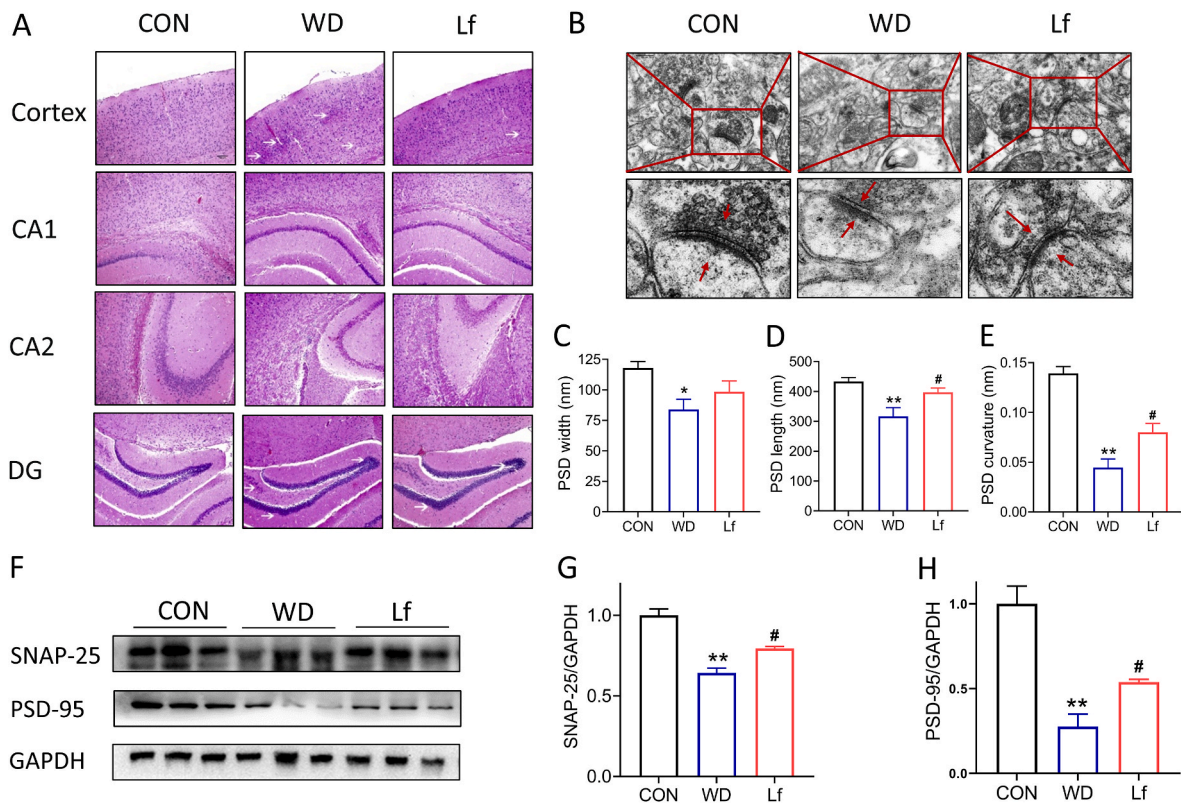


**Fig. 3.** Lf intervention improved the hippocampal neurons and synapses in mice fed with 'Western'-style diets (WD). A. histopathology of mouse brain; B. representative image of ultrastructure of synapse in the hippocampus by transmission electron microscope (TEM); C. postsynaptic density proteins (PSD) width; D. PSD length; E) PSD curvature (n = 6 mice each group); F. representative western blots of synaptosomal associated proteins 25 (SNAP-25) and PSD-95.; G. quantitative measurement of SNAP-25; H. quantitative measurement of PSD-95 (n = 3 mice each group). \*P < 0.05 vs. the CON group; \*\*P < 0.01 vs. the CON group. #P < 0.05 vs., the WD group; ##P < 0.01 vs. the WD group.

### 3.7. Lf intervention improved gut microbiota alteration

The effects of Lf on the community structure of the gut microbiota were investigated by 16S rRNA gene-based profiling of fecal microbiota. The  $\alpha$  diversity of the gut microbiota was assessed by Chao 1, Shannon indices, and ACE, all of which reflect species richness. Compared with the CON group, the WD group presented a decrease in  $\alpha$  diversity in the gut microbiota. Meanwhile, Lf intervention significantly increased the mean community diversity indices (Chao1 and Shannon) compared with those in the WD group (Fig. 7A–C). Principal coordinate analysis (PCoA) of the colonic microbiota community revealed a separated microbial cluster of three groups, and the unweighted unifrac test indicated that the abundance of the gut microbiota accounted for 42.33% and 11.08% difference of the total variations. (Fig. 7D and E). Figs. A.2 shows the differences among the three groups at the phylum, class, and family levels, respectively. Firmicutes, Bacteroidetes, Deferribacteres, and Proteobacteria were the dominant bacteria at the phylum level. Clostridia, Bacteroidia, Deferribacteres, and Deltaproteobacteria were the dominant bacteria at the class level. Ruminococcaceae, S24-7, Lachnospiraceae, and Desulfobivibrionaceae were the dominant bacteria at the family level. WD feeding significantly decreased the relative abundance of Bacteroidetes and Proteobacteria and increased Firmicutes compared with those in the CON group. However, Lf restored the abundance of Bacteroidetes and Proteobacteria to the level in the CON group. WD feeding increased Firmicutes/Bacteroidetes (F/B) ratio, which was reversed by Lf intervention, although no significant difference was observed among the three groups (Fig. 7F). LEfSe analysis indicated that bacteria belonging to the Firmicutes phylum, Tenericutes class, Clostridiales order, and *Roseburia* genus differentially enriched the gut bacterial communities (Linear discriminant analysis score >3) of the

CON and WD groups (Fig. 7G and H). Lf intervention regulated the WD-induced shift in microbiome composition by increasing the relative abundances of Bacteroidetes phylum and *Roseburia* genus (Fig. 7I and J). Further analysis was conducted on the relationship between the gut microbiota and behavior test results using Spearman's correlation. Cognitive function was positively correlated with phylum Bacteroidetes and Verrucomicrobia, and genus *Odoribacter*, but negatively correlated with phylum Proteobacteria and Actinobacteria, and genus *AF 12* (Fig. A2).

### 3.8. Antibiotics eliminated the benefit of long-term Lf intervention in cognitive impairment

A cocktail of oral antibiotics led to a 20-fold reduction in fecal bacterial load (Fig. 8A). WD feeding increased body weight and white adipose tissue weight. Compared with those in the Lf group, the mice in the Lf + AB group gained more body weight and had heavier subcutaneous fat at autopsy (Fig. 8B and C). Meanwhile, the indexes of behavioral tests in the Lf + AB group were significantly different from the CON group, and no significantly different from the WD group. Meanwhile, the nesting score was significantly lower in the Lf + AB group than in the Lf group (Fig. 8D). Although no significant differences were found between the two groups, exploration time with a novel object, the number of head exploration and crossing number were decreased and escape latency were increased in the Lf + AB group (Fig. 8E–H). Thus, the cognitive improvement effect of Lf tended to disappear when the gut microbiota was removed.

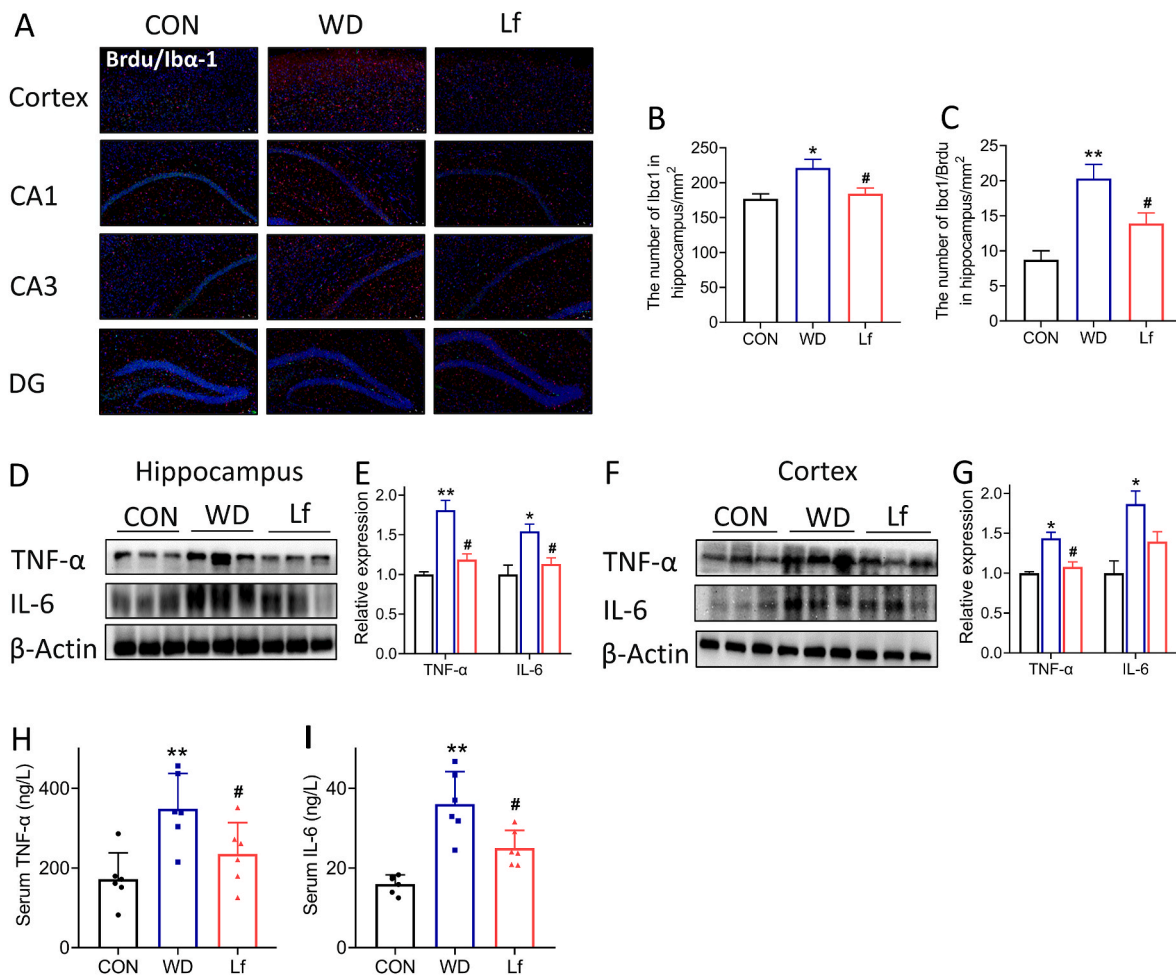


**Fig. 4.** Lf intervention suppressed 'Western'-style diets (WD)-induced microglia activation and inflammation in the mouse brain and serum. A. representative immunofluorescence double staining of Iba1 and BrdU; B. the number of Iba1 in hippocampus; C. the number of Iba1/BrdU in hippocampus. D. representative western blots of TNF- $\alpha$  and IL-6 in the hippocampus, and E. the quantitative measurement; F. representative western blots of TNF- $\alpha$  and IL-6 in the cortex, and G. their quantitative measurement (n = 3 mice each group); H. serum TNF- $\alpha$ ; I. serum IL-6 (n = 6 mice each group). \*P < 0.05 vs. the CON group; \*\*P < 0.01 vs. the CON group. #P < 0.05 vs., the WD group; ##P < 0.01 vs. the WD group.

### 3.9. Short-term Lf intervention prevented WD-induced gut microbiota alteration prior to the cognitive behavioral changes

The behavior tests and gut microbiota were analyzed at 2 weeks after intervention. We found that Lf intervention for 2 weeks did not affect cognitive function in the WD-fed mice based on the behavior tests (Fig. 9A-E). However, WD feeding decreased the  $\alpha$  diversity in the gut microbiota, which was partly restored by Lf intervention (Fig. 9F-H). PCoA analysis showed that the gut microbial profile in the Lf group was separately clustered from that in the WD group (Fig. 9H). Furthermore, the increased proportion of Firmicutes and decreased proportion of Bacteroidetes in the WD group were restored by Lf intervention (Fig. 9J). In other word, short-term Lf intervention modulated the gut microbial profile and did not affect cognitive function, suggesting that Lf resulted in gut microbiota alteration before the cognitive function changes.

## 4. Discussion

Accumulating evidence indicates that WD high in fat and sugar impairs cognitive function (O'Brien et al., 2017; Kendig et al., 2021). The imbalance in the microbiome-gut-brain axis may negatively affect cognitive function (Buford, 2017; Leigh and Morris, 2020). Lf prevents memory impairment and influences gut microbiota (Abdelhamid et al., 2020; Tsatsanis et al., 2021; Zhou et al., 2021), but its association with

gut microbial dysbiosis in cognitive impairment is less well-established. In this study, WD feeding for 16 weeks resulted in cognitive impairment and gut microbial dysbiosis in mice. In addition, antibiotics partly eliminated the effects of long-term Lf intervention on cognitive impairment, suggesting that the gut microbiota participated in Lf action. However, the degree to which gut microbiota may affect cognitive function should be further investigated. On the other hand, a short-term Lf intervention was performed to resolve the space in the microbiome-gut-brain axis. We found that Lf intervention for two weeks prevented WD-induced gut microbiota alteration without inducing behavioral changes, thus supporting the timing sequence of gut microbiota to the brain. Thus, Lf intervention is likely to ameliorate cognitive impairment by improving the gut-microbiome-gut-brain axis.

At first, the bioavailability of Lf should be considered since dietary protein is hydrolyzed to small molecule peptide and amino acids in the digestive system for absorption and utilization, and only very few proteins are directly absorbed in their original form. After oral administration of (125)I-labeling Lf, only functional fragments of Lf survived proteolytic degradation and were detected in mouse small intestine (Kuwata et al., 2001). However, another animal study found that Lf resists major proteolytic degradation in the intestinal lumen and is readily absorbed in an antigenic form in mouse blood (Fischer et al., 2007). On the other hand, a clinical trial observed that Lf intake did not affect the volunteers' serum Lf content, suggesting that human could not

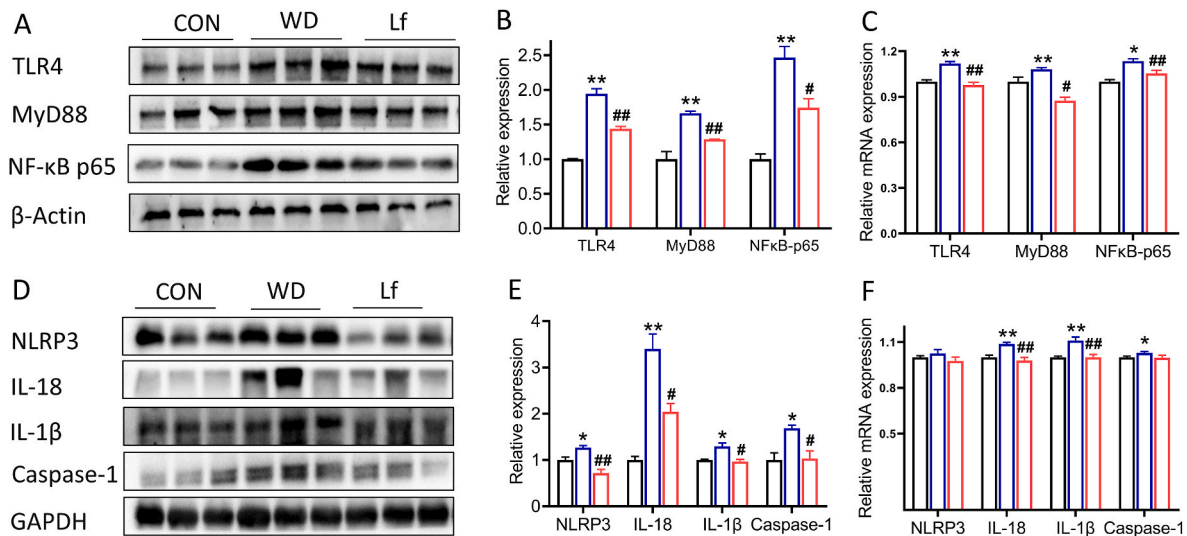


**Fig. 5.** Lf intervention inhibited the 'Western'-style diets (WD)-induced activation of toll-like receptor 4 (TLR4)/nuclear factor kappa-B (NF-κB) signaling pathway and NOD-like receptor thermal protein domain associated protein 3 (NLRP3) inflammasomes in the mouse hippocampus. A. representative western blots of TLR4, MyD88 and NF-κB p65, and B. the quantitative measurement; C. the mRNA expression. D. representative western blots of NLRP3, IL-18, IL-1β and caspase-1, and E. quantitative measurement; F. the mRNA expression; (n = 3 mice each group). \*P < 0.05 vs. the CON group; \*\*P < 0.01 vs. the CON group. #P < 0.05 vs., the WD group; ##P < 0.01 vs. the WD group.

directly absorb Lf into the circulatory system (Hayes et al., 2006). However, another study reported that less than 40% of Lf was digested and degraded in the stomach in young adults (Furlund et al., 2013). Thus, both animal studies and human trials did not yielded consistent results regarding the Lf bioavailability. Lf degradation and peptide formation after gastric and duodenal digestion were highly dependent on gastric pH and gastrointestinal environment. In real life, oral intake is more common and reasonable for nutrients intervention. Intragastrical administration of Lf was selected in the present animal study.

In the present study, the nesting behavior test, NOR test, and MWM test were performed to explore hippocampus-dependent recognition memory and the ability to perform activities of daily living (Bevins and Besheer, 2006; Deacon, 2006; Vorhees and Williams, 2006). The findings showed that Lf inhibited the WD-induced detriment of working learning and memory ability. Aging may reduce spatial learning ability and impair spatial memory retrieval ability. Using the MWM test, Zheng et al. (2020) found that Lf gavage for 3 months partially restored spatial cognition in 16-month-old C57/BL6J mice. Abdelhamid et al. used the preference index to measure cognitive function in NOR tests and found that both Lf and hydrolyzed Lf feeding for 3 months induced a preference for novel objects in APP-Tg mice (Abdelhamid et al., 2020). Xu et al. (2019) also found that peritoneally Lf injection for 1 week substantially ameliorated PD-like motor dysfunction in mouse model. Thus, Lf benefits the impaired cognitive function in various animal models of neurodegenerative diseases.

The findings were further demonstrated in the hippocampus, which is involved in cognitive processing, learning, and memory. The dysregulation of synaptic formation and plasticity in the hippocampus has been implicated in cognitive impairment and AD (Lamont and Weber, 2012). As expected, WD disrupted the hippocampal ultrastructural synaptic architecture and Lf effectively reversed the morphological damage of postsynaptic density. PSD-95 is a member of the PSD family and plays an important role in synaptic integration and neural function recovery (Ugalde-Trivino and Diaz-Guerra, 2021). SNAP-25 is a member of the receptor family of soluble N-ethyl maleimide sensitive factor attachment proteins and regulates the extracellular secretion of synaptic vesicles (Shaaban et al., 2019). This study demonstrated that Lf significantly upregulated the expression of synaptic functional proteins SNAP-25 and PSD-95 in the hippocampus. Together with the results on related protein expression, this finding supported that Lf retard the

WD-induced impairment of cognitive function.

Obesity-related diseases are characterized by chronic inflammation. In the present study, Lf significantly decreased the body weight and white adipose tissues, and improved the WD-induced dyslipidemia. The mitigation of obese status by Lf was linked to inflammation inhibition and immunoregulation in the brain. Microglia are the resident immune cells of the brain that become activated in response to infections and other injuries. Excessive microglial activation can damage the surrounding healthy neural tissues. In turn, the factors secreted by the dead or dying neurons exacerbate the chronic activation of microglia, causing progressive loss of neurons, and subsequent cognitive impairment (Bao et al., 2018). Immunofluorescence analysis showed that Lf inhibited WD-induced microglial activation in the hippocampal regions. Activated microglia produce a wide spectrum of proinflammatory cytokines, which ultimately induce neuronal damage (Banati, 2002). Similarly, Lf intervention downregulated the expression of TNF-α and IL-6 in the cortex and hippocampus. On the other hand, circulation cytokines can reach the brain via the cytokine transporters expressed by the endothelial cells of the blood-brain barrier and subsequently modulate the cytokine production of microglia (Bairamian et al., 2022). Zheng et al. (2020) found that Lf reduced the hippocampal and serum levels of IL-1β, IL-6, and TNF-α in aged mice. In the present study, the cross-talk of peripheral and central inflammation was observed because Lf simultaneously alleviated the serum levels of TNF-α and IL-6.

As the first-line host defense against invading pathogens on the surface of microglia, TLR4 activates multiple downstream signaling pathways, such as NF-κB signaling pathways (Lu et al., 2008). After binding with Aβ, TLR4 can activate the NF-κB complex and downstream events that participate in the transcriptional expression of NLRP3 and pro-IL-β (Zhou et al., 2014). In normal inflammatory cells, activated TLR4 can bind directly to intracellular protein myeloid differentiation factor MyD88. MyD88 upregulation can further increase the expression of inflammatory cytokines such as TNF-α and IL-1β (Zhao et al., 2014). On the other hand, NF-κB mediates the formation of NLRP3 inflammasome, which recruits and polymerizes ASC, leading to caspase-1 activation. An activated caspase-1 promotes the maturity and release of pro-inflammatory cytokines (Yu et al., 2022). As a result, numerous neuroinflammation processes further exacerbate the pathological processes that cause cognitive impairment (Holmes, 2013). In this study, NF-κB/NLRP3 inflammasome activation mediated neuroinflammation

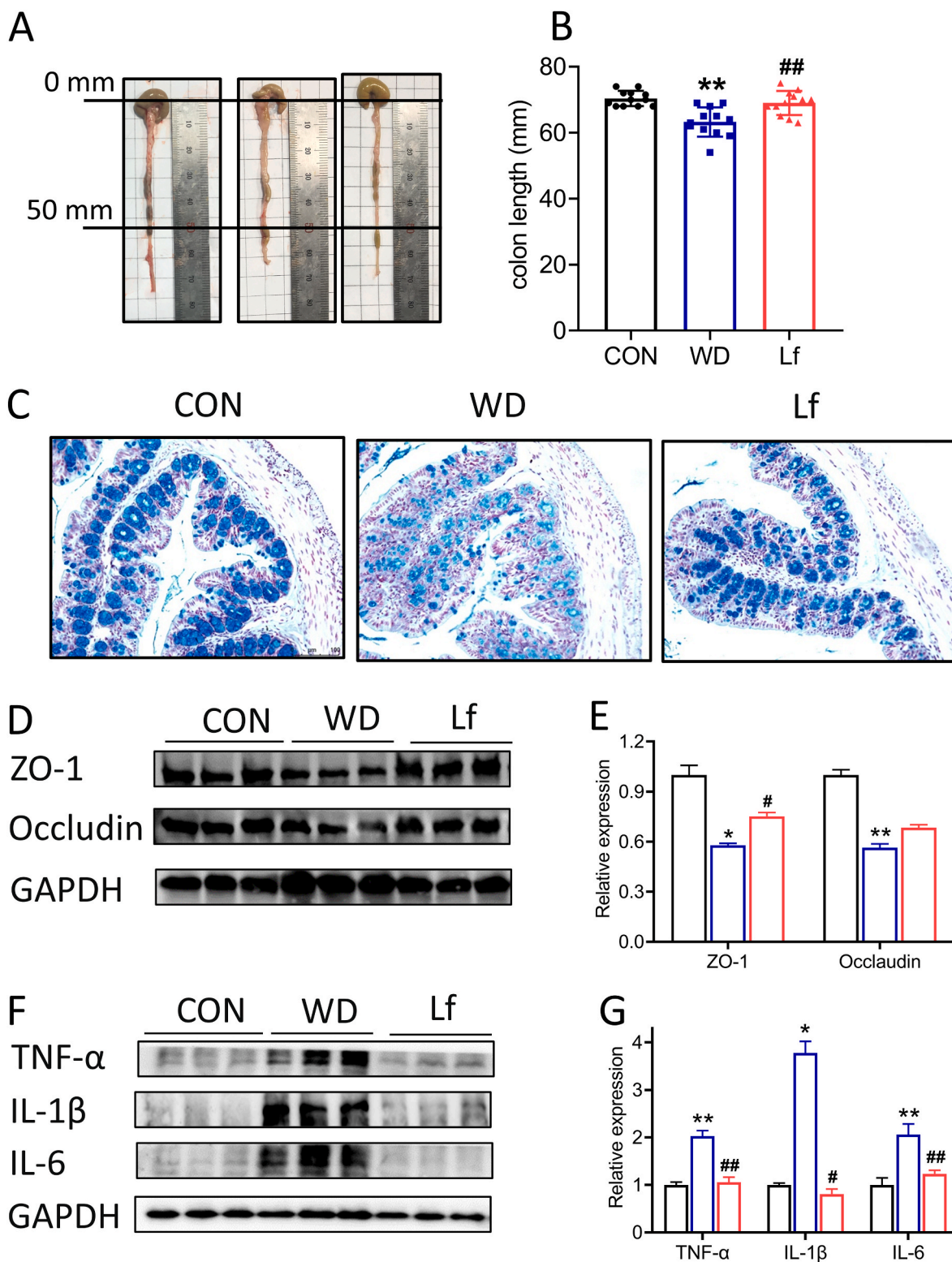


**Fig. 6.** Lf intervention maintained colonic integrity and alleviated inflammation in mice fed with 'Western'-style diets (WD). A. representative images of colons, and B. the quantification of colon length; C. Alcian blue-stained colonic sections; D. representative western blots of ZO-1 and occludin in the mice colon, and E. quantitative measurement; F. representative western blots of TNF- $\alpha$ , IL-1 $\beta$  and IL-6 in the mice colon, and G. quantitative measurement (n = 3 mice each group). \*P < 0.05 vs. the CON group; \*\*P < 0.01 vs. the CON group. #P < 0.05 vs. the WD group; ##P < 0.01 vs. the WD group. (For interpretation of the references to color in this figure legend, the reader is referred to the Web version of this article.)

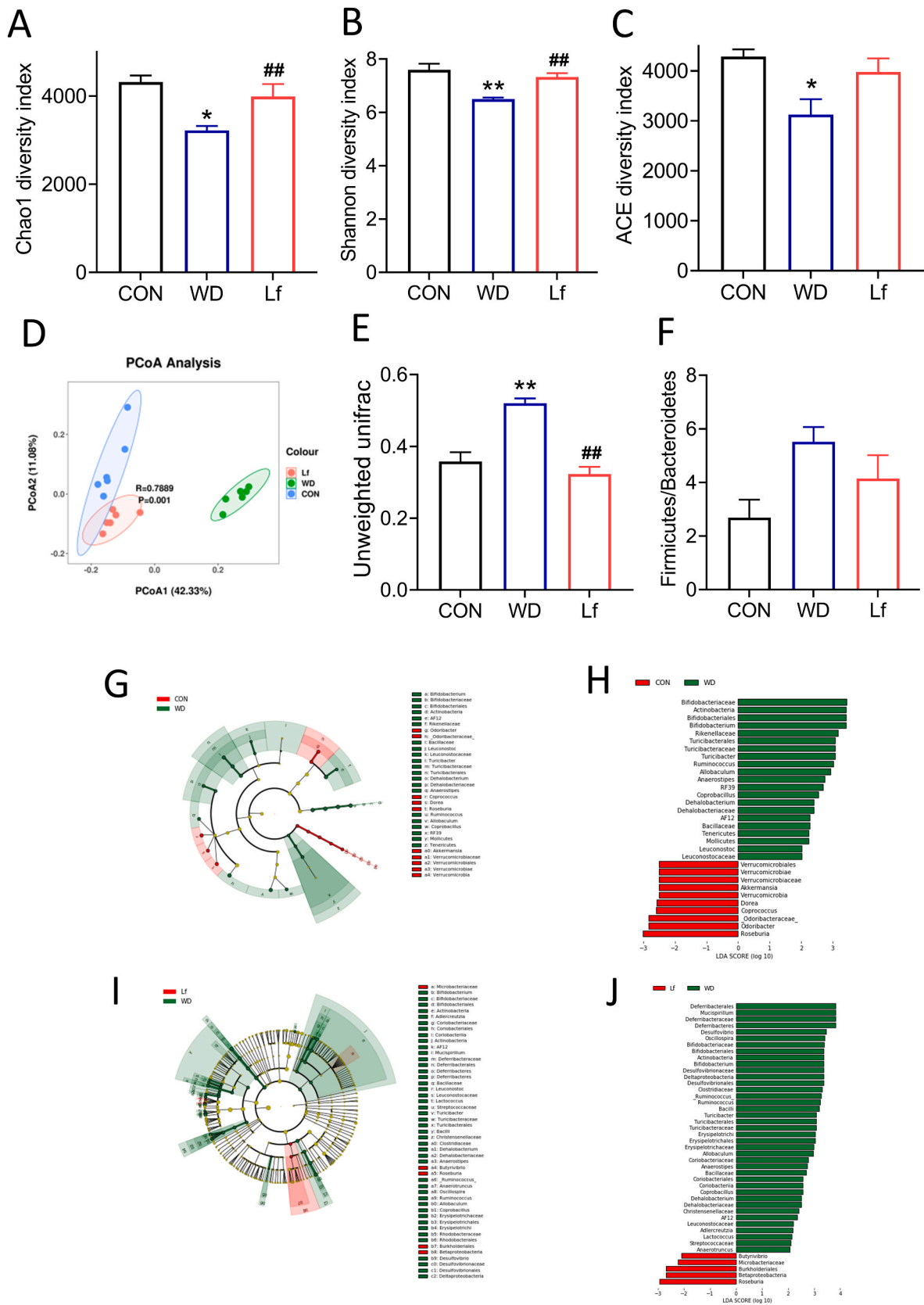


**Fig. 7.** Lf intervention influenced gut microbiota alteration in mice fed with 'Western'-style diets (WD). **A.** Chao 1 diversity index; **B.** Shannon diversity index; **C.** abundance-based coverage estimator (ACE) diversity index; **D.** principal coordinates analysis (PCoA) based on unweighted UniFrac distances; **E.** unweighted UniFrac distances; **F.** the ratio of Proteobacteria/Bacteroidetes; **G,H.** linear discriminant analysis effect size (LEfSe) showing the most differentially significant abundant taxa enriched in microbiota from the CON and WD; **I,J.** LEfSe showing the most differentially significant abundant taxa enriched in microbiota from the Lf and WD (n = 6 mice each group); \*P < 0.05 vs. the CON group; \*\*P < 0.01 vs. the CON group. ##P < 0.05 vs., the WD group; ###P < 0.01 vs. the WD group.

## Bacteria level and body/fat weight

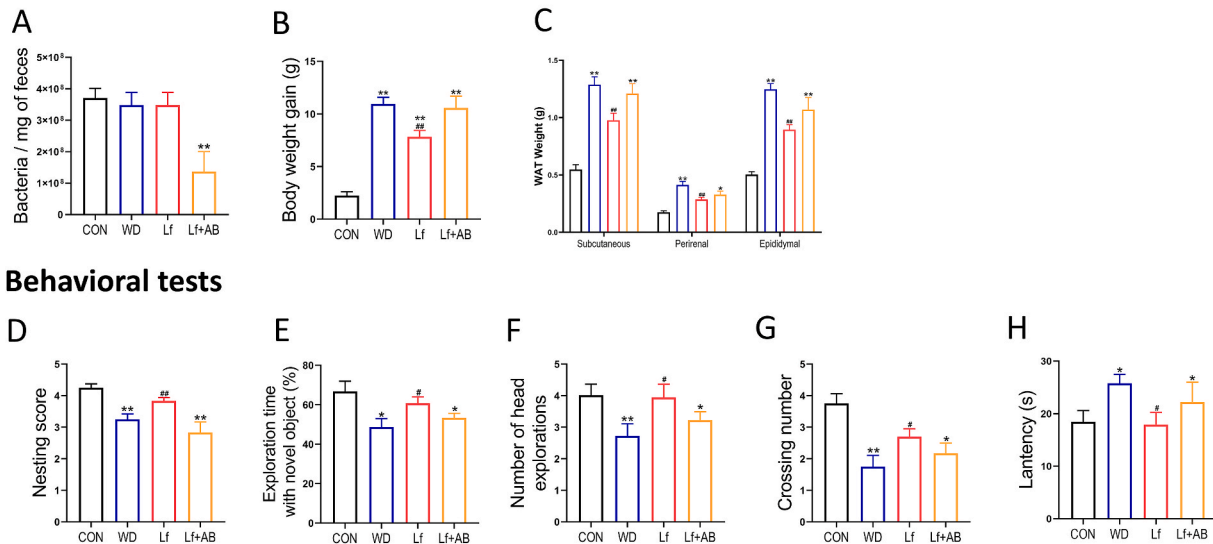
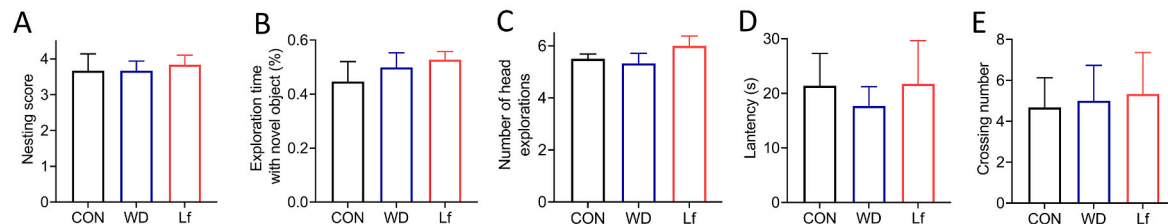


**Fig. 8.** Antibiotics eliminated the effects of long-term Lf intervention in abrogating inflammation and cognitive impairment. A. bacteria level; B. body weight gain; C. WAT weight; D-H. behavioral tests. D. the nest scores in the nesting behavior test; E. percentage of time spent with the novel object, and F. the number of head explorations in the novel object recognition (NOR) test; G. crossing number in the Morris water maze (MWM) test, and H. escape latency. (n = 6 mice each group). \*P < 0.05 vs. the CON group; \*\*P < 0.01 vs. the CON group. #P < 0.05 vs., the WD group; ##P < 0.01 vs. the WD group. \$p < 0.05, \$\$p < 0.01 vs. Lf group.

## Behavioral tests



## Gut microbiota

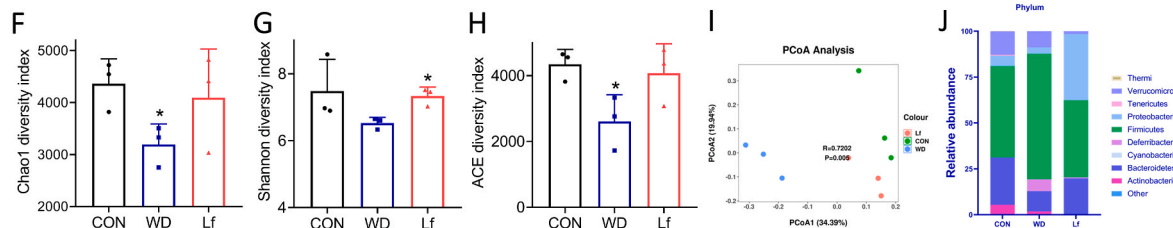


**Fig. 9.** Lf intervention for 2 weeks prevented 'Western'-style diets (WD)-induced gut microbiota alteration prior to the behavioral cognitive changes. A. the nest scores in the nesting behavior test; B. percentage of time spent with the novel object, and C. the number of head explorations in the novel object recognition (NOR) test; D. escape latency, and E. crossing number in the Morris water maze (MWM) test. (n = 6 mice each group); F. Chao 1 diversity index; G. Shannon diversity index; H. ACE diversity index; I. PCoA based on unweighted UniFrac distances; J. relative abundance (n = 3 mice each group). \*P < 0.05 vs. the CON group; \*\*P < 0.01 vs. the CON group. #P < 0.05 vs., the WD group; ##P < 0.01 vs. the WD group.

caused by WD feeding. Lf intervention inhibited the WD-induced upregulation of the NF- $\kappa$ B/NLRP3/caspase-1/IL-1 $\beta$ /IL-18 axis. The benefit of Lf on NF- $\kappa$ B/NLRP3 inflammasome was previously observed on other cells or organ injury. Nemati et al. demonstrated that Lf downregulated TLR4, MyD88, IL-6, and TNF- $\alpha$  expression in lipopolysaccharide-activated murine RAW264.7 cells (Nemati et al., 2021). Madkour et al. (2022) found that Lf administration significantly ameliorated glycerol-induced rhabdomyolysis and acute kidney injury by decreasing renal IL-1 $\beta$ , NLRP3 and NF- $\kappa$ B. As far as we know, the present study is the first to demonstrate that the anti-inflammation effects of Lf may be related to its inhibition of NF- $\kappa$ B/NLRP3

inflammasome activation in the hippocampus.

Impaired gut permeability allows for the influx of adverse substances and disrupts the gut bacterial ecosystem (Malesza et al., 2021). Obese-type microbiota transplantation disrupts intestinal barrier function and induces a cognitive decline in mice (Bruce-Keller et al., 2015). In this study, WD diet intake dramatically increased intestinal inflammation and diminished intestinal barrier integrity, which was consistent with previous studies (Tsatsanis et al., 2021). Lf intervention increased colon length, upregulated colonic tight-junction protein occludin, and lowered colonic inflammation. Similarly, Hu et al. (2022) found that Lf treatment restored the deoxyvalenol induced damage of mouse

intestinal integrity by enhancing the occludin expression and reducing the production of proinflammatory cytokines.

The gut microbiota exerts its action partly by modulating neuroinflammation. Microglia, which are involved in neuroinflammation development, are mediated by the gut microbiota (Bairamian et al., 2022). Altered gut microbiota was positively correlated with microgliosis and increased cerebral NLRP3 inflammasome and IL-1 $\beta$  in a mouse model of AD (Shukla et al., 2021). Transplantation of the gut microbiota of AD patients induced the activation of NLRP3 inflammasome and caused the release of inflammatory factors in the intestinal tract of mice (Shen et al., 2020). By contrast, the transplantation of healthy fecal microbiota protected the PD mice by suppressing neuroinflammation and inhibiting TLR4/TNF- $\alpha$  signaling pathway (Sun et al., 2018). In the present study, Lf restored the WD-induced decrease in the  $\alpha$  diversity of the gut microbiota, which was consistent with the findings of other studies using suckling piglets and APP/PS1 mice (Hu et al., 2020; Zhou et al., 2021). Thus, the observed benefits of Lf on cognitive impairment, neuroinflammation, and NF- $\kappa$ B/NLRP3 inflammasomes in the hippocampus are possibly linked to the gut microbiota.

Bacteroidetes are beneficial for the gut barrier (Desai et al., 2016). In a cross-sectional study, a low Bacteroidetes abundance was found in the gut microbiota of dementia patients (Saji et al., 2019). In the present study, Lf restored the WD-induced decrease in Bacteroidetes and improved epithelial damage and memory impairment. Correlation analysis further indicated that cognitive function was positively correlated with Bacteroidetes. Therefore, Lf regulated Bacteroidetes in the microbiome-gut-brain axis to alleviate cognitive impairment. F/B ratio is significantly increased in obese mice (Koliada et al., 2017). In humans, the F/B ratio increases several folds with aging, a major risk of neurodegenerative diseases (Ley et al., 2006). In the present study, Lf intervention tended to decrease the F/B ratio, which was consistent with other study using high-fat diet mice treated with Lf (Li et al., 2022). *Roseburia* genus is associated with obesity and neurodegenerative diseases (Karlsson et al., 2013; Keshavarzian et al., 2015). A systematic search found that *Roseburia* is the lean-associated genus in the Eastern population (Xu et al., 2022). Hu et al. (2020) found that suckling piglets that drank Lf-containing solution had a high *Roseburia* abundance. In the present study, Lf intervention increased the abundance of *Roseburia*, which is probably linked to improved cognitive impairment.

## 5. Conclusion

Overall, our findings demonstrated the beneficial effects of Lf

intervention on the cognitive impairment of WD-induced obese mice by alleviating synaptic damages and inhibiting microglial activation. The underlying mechanism may involve decreased neuroinflammation by inhibiting the activation of NF- $\kappa$ B/NLRP3 inflammasomes and ameliorating the shift in gut microbiota composition through the microbiome-gut-brain axis. More well-designed experiments are warranted to elucidate the complex interplay of gut microbiota, inflammation, and cognitive function.

## CRedit authorship contribution statement

**Qian He:** Conceptualization, Data curation, Formal analysis, Investigation, Methodology, Project administration, Writing – original draft, preparation. **Li-Li Zhang:** Investigation, Formal analysis, Validation, Project administration. **Deming Li:** Investigation, Project administration. **Jiangxue Wu:** Investigation. **Ya-Xin Guo:** Investigation. **Jingbo Fan:** Investigation. **Qingyang Wu:** Investigation. **Hai-Peng Wang:** Conceptualization, Investigation, Funding acquisition. **Zhongxiao Wan:** Methodology, Writing – review & editing. **Jia-Ying Xu:** Conceptualization, Validation, Funding acquisition, Writing – review & editing. **Li-Qiang Qin:** Conceptualization, Investigation, Methodology, Data curation, Writing – original draft, Writing – review & editing, Supervision, Funding acquisition.

## Declaration of competing interest

On behalf of all authors, the corresponding author states that there is no conflict of interest.

## Data availability

Data will be made available on request.

## Acknowledgements

This work was supported by the National Natural Science Foundation of China (no. 82173502, and 81973024), Key Laboratory Open Project for State Key Laboratory of Radiation Medicine and Protection, China (GZK1202001), and Priority Academic Program Development of Jiangsu Higher Education Institutions (PAPD), China.

## Appendix

**Table A.1**  
Diet Ingredients

ingredient	Standard diet(grams/kg)	WD (grams/kg)
Casein	200	195
DL-Methionine (DL)		3
L-Cystine	3	
Sucrose	100	410
Cornstarch	389.486	
Maltodextrin 10		81
Dyetrose	132	
Milkfat		20
Ethoxyquin		0.04
Corn oil		10
Soybean oil	70	
Cellulose	50	
Mineral Mix #20000	35	35
Vitamin Mix # 300050	10	10
Choline Bitartrate	2.5	2
Cholesterol		12.66
Kcal/g	4	4.63

**Table A.2**  
Paired primers for *qRT-PCR* analysis

Gene	Primer sequence (5'-3')	
	Forward	Reverse
NLRP3	GTGGTGACCCTCTGTGAGGT	TCTTCCTGGAGCGCTTCTAA
IL-18	CAATGGTTCCTTCATTGAGC	AACAAACAGGAGAAGTTGGT
IL-1 $\beta$	TCAGGCAGGCAGTATCACTC	CATGAGTCACAGAGGATGGG
Caspase-1	ACAAGGCACGGGACCTATG	TCCCAGTCAGTCCTGGAAATG
TLR4	CTGGGTGAGAAAGCTGGTAA	AGCCTTCCTGGATGATGTTGG
MyD88	TATACCAACCTTGACACCAAGTC	TCAGGCTCCAAGTCAGCTCATC
NF- $\kappa$ B	CCAAAGAAGGACACGACAGAATC	GGCAGGCTATTGCTCATCACA
ZO-1	CACACGATGCTCAGAGACGAAGG	CTGTATGGTGGCTGCTCAAGGTC
Occludin	GACCTTGTCGGTGGATGACTTCAG	ATCAGCAGCAGCCATGTACTCTTC
TNF- $\alpha$	GGCGTGTTCATCCGTTCTC	CTTCAGCGTCTCGTGTGTTTC
IL-6	ATTGTATGAACAGCGATGATGCAC	CCAGGTAGAAACGGAACCTCAGA
Gapdh	ATGACTCTACCCACGGCAAG	GATCTCGCTCTGGAAGATG

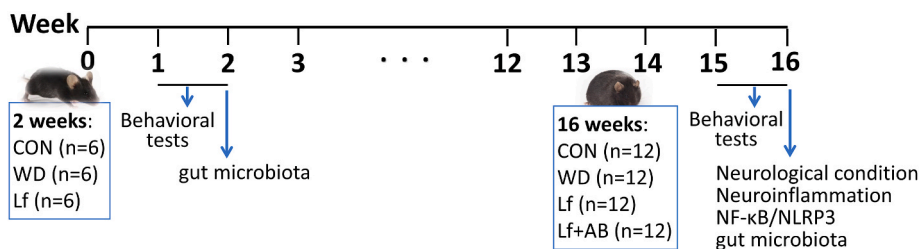


**Fig. A1.** The experimental design.

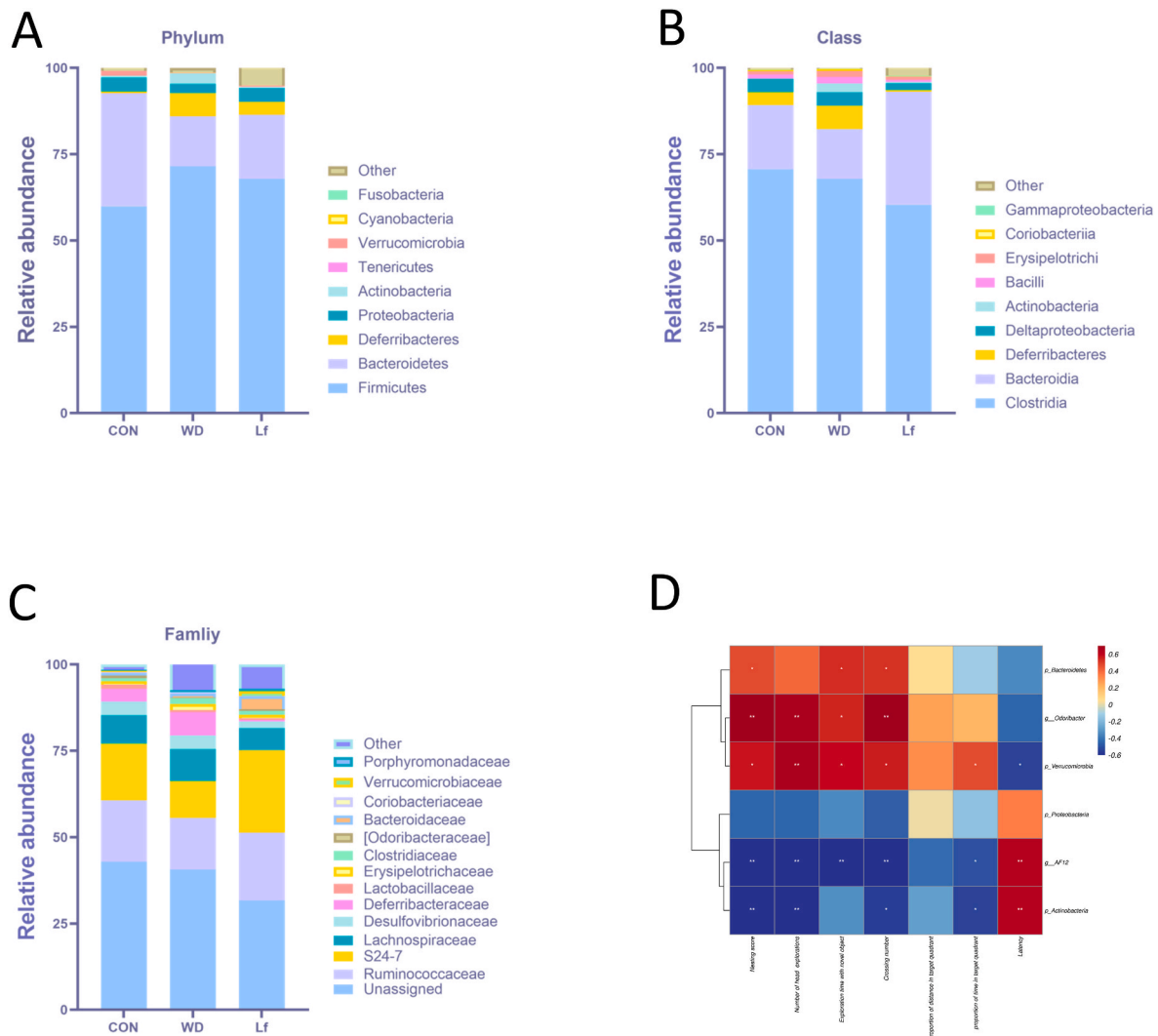


**Fig. A2.** A-C. taxonomic distribution of relative abundance of microbiota at the phylum, class and family levels; D. correlation between the gut microbiota and behavior test results.

## References

- Abdelhamid, M., Jung, C.G., Zhou, C., Abdullah, M., Nakano, M., Wakabayashi, H., Michikawa, M., 2020. Dietary lactoferrin supplementation prevents memory impairment and reduces amyloid-beta generation in J20 mice. *J Alzheimers Dis* 74 (1), 245–259. <https://doi.org/10.3233/JAD-191181>.
- Bairamian, D., Sha, S., Rolhion, N., Sokol, H., Dorothee, G., Lemere, C.A., Krantic, S., 2022. Microbiota in neuroinflammation and synaptic dysfunction: a focus on Alzheimer's disease. *Mol. Neurodegener.* 17 (1), 19. <https://doi.org/10.1186/s13024-022-00522-2>.
- Banati, R.B., 2002. Visualising microglial activation in vivo. *Glia* 40 (2), 206–217. <https://doi.org/10.1002/glia.10144>.
- Bao, L.H., Zhang, Y.N., Zhang, J.N., Gu, L., Yang, H.M., Huang, Y.Y., Zhang, H., 2018. Urate inhibits microglia activation to protect neurons in an LPS-induced model of Parkinson's disease. *J. Neuroinflammation* 15 (1), 131. <https://doi.org/10.1186/s12974-018-1175-8>.
- Bauernfeind, F.G., Horvath, G., Stutz, A., Alnemri, E.S., MacDonald, K., Speert, D., Latz, E., 2009. Cutting edge: NF-kappaB activating pattern recognition and cytokine receptors license NLRP3 inflammasome activation by regulating NLRP3 expression. *J. Immunol.* 183 (2), 787–791. <https://doi.org/10.4049/jimmunol.0901363>.
- Bevins, R.A., Besheer, J., 2006. Object recognition in rats and mice: a one-trial non-matching-to-sample learning task to study 'recognition memory'. *Nat. Protoc.* 1 (3), 1306–1311. <https://doi.org/10.1038/nprot.2006.205>.
- Boscaini, S., Cabrera-Rubio, R., Speakman, J.R., Cotter, P.D., Cryan, J.F., Nilaweera, K. N., 2019. Dietary alpha-lactalbumin alters energy balance, gut microbiota composition and intestinal nutrient transporter expression in high-fat diet-fed mice. *Br. J. Nutr.* 121 (10), 1097–1107. <https://doi.org/10.1017/S0007114519000461>.
- Brimelow, R.E., West, N.P., Williams, L.T., Cripps, A.W., Cox, A.J., 2017. A role for whey-derived lactoferrin and immunoglobulins in the attenuation of obesity-related inflammation and disease. *Crit. Rev. Food Sci. Nutr.* 57 (8), 1593–1602. <https://doi.org/10.1080/10408398.2014.995264>.
- Bruce-Keller, A.J., Salbaum, J.M., Luo, M., Blanchard, E. th, Taylor, C.M., Welsh, D.A., Berthoud, H.R., 2015. Obese-type gut microbiota induce neurobehavioral changes in the absence of obesity. *Biol. Psychiatr.* 77 (7), 607–615. <https://doi.org/10.1016/j.biopsych.2014.07.012>.
- Buford, T.W., 2017. Dis)Trust your gut: the gut microbiome in age-related inflammation, health, and disease. *Microbiome* 5 (1), 80. <https://doi.org/10.1186/s40168-017-0296-0>.
- Cheng, X., Yeung, P.K.K., Zhong, K., Zilundu, P.L.M., Zhou, L., Chung, S.K., 2019. Astrocytic endothelin-1 overexpression promotes neural progenitor cells proliferation and differentiation into astrocytes via the Jak2/Stat3 pathway after stroke. *J. Neuroinflammation* 16 (1), 227. <https://doi.org/10.1186/s12974-019-1597-y>.
- Deacon, R.M., 2006. Assessing nest building in mice. *Nat. Protoc.* 1 (3), 1117–1119. <https://doi.org/10.1038/nprot.2006.170>.
- Desai, M.S., Seekatz, A.M., Koropatkin, N.M., Kamada, N., Hickey, C.A., Wolter, M., Martens, E.C., 2016. A dietary fiber-deprived gut microbiota degrades the colonic mucus barrier and enhances pathogen susceptibility. *Cell* 167 (5), 1339–1353 e1321. <https://doi.org/10.1016/j.cell.2016.10.043>.
- Diaz Heijtz, R., Wang, S., Anuar, F., Qian, Y., Bjorkholm, B., Samuelsson, A., Pettersson, S., 2011. Normal gut microbiota modulates brain development and behavior. *Proc. Natl. Acad. Sci. U. S. A.* 108 (7), 3047–3052. <https://doi.org/10.1073/pnas.1010529108>.
- Dinel, A.L., Andre, C., Aubert, A., Ferreira, G., Laye, S., Castanon, N., 2014. Lipopolysaccharide-induced brain activation of the indoleamine 2,3-dioxygenase and depressive-like behavior are impaired in a mouse model of metabolic syndrome. *Psychoneuroendocrinology* 40, 48–59. <https://doi.org/10.1016/j.psyneuen.2013.10.014>.

- Fan, J.G., Kim, S.U., Wong, V.W., 2017. New trends on obesity and NAFLD in Asia. *J. Hepatol.* 67 (4), 862–873. <https://doi.org/10.1016/j.jhep.2017.06.003>.
- Farruggia, M.C., Small, D.M., 2019. Effects of adiposity and metabolic dysfunction on cognition: a review. *Physiol. Behav.* 208, 112578. <https://doi.org/10.1016/j.physbeh.2019.112578>.
- Fischer, R., Debbabi, H., Blais, A., Dubarry, M., Rautureau, M., Boyaka, P.N., Tome, D., 2007. Uptake of ingested bovine lactoferrin and its accumulation in adult mouse tissues. *Int. Immunopharm.* 7 (10), 1387–1393. <https://doi.org/10.1016/j.intimp.2007.05.019>.
- Fung, T.C., Olson, C.A., Hsiao, E.Y., 2017. Interactions between the microbiota, immune and nervous systems in health and disease. *Nat. Neurosci.* 20 (2), 145–155. <https://doi.org/10.1038/nn.4476>.
- Furlund, C.B., Ulleberg, E.K., Devold, T.G., Flengsrud, R., Jacobsen, M., Sekse, C., Vegarud, G.E., 2013. Identification of lactoferrin peptides generated by digestion with human gastrointestinal enzymes. *J. Dairy Sci.* 96 (1), 75–88. <https://doi.org/10.3168/jds.2012-5946>.
- Guo, C., Yang, Z.H., Zhang, S., Chai, R., Xue, H., Zhang, Y.H., Wang, Z.Y., 2017. Intranasal lactoferrin enhances alpha-secretase-dependent Amyloid precursor protein processing via the ERK1/2-CREB and HIF-1alpha pathways in an Alzheimer's disease mouse model. *Neuropsychopharmacology* 42 (13), 2504–2515. <https://doi.org/10.1038/npp.2017.8>.
- Hayes, T.G., Falchook, G.F., Varadhachary, G.R., Smith, D.P., Davis, L.D., Dhingra, H.M., Varadhachary, A., 2006. Phase I trial of oral talactoferrin alfa in refractory solid tumors. *Invest. N. Drugs* 24 (3), 233–240. <https://doi.org/10.1007/s10637-005-3690-6>.
- Holmes, C., 2013. Review: systemic inflammation and Alzheimer's disease. *Neuropathol. Appl. Neurobiol.* 39 (1), 51–68. <https://doi.org/10.1111/j.1365-2990.2012.01307.x>.
- Hu, P., Zhao, F., Wang, J., Zhu, W., 2020. Early-life lactoferrin intervention modulates the colonic microbiota, colonic microbial metabolites and intestinal function in suckling piglets. *Appl. Microbiol. Biotechnol.* 104 (14), 6185–6197. <https://doi.org/10.1007/s00253-020-10675-z>.
- Hu, P., Zong, Q., Zhao, Y., Gu, H., Liu, Y., Gu, F., Cai, D., 2022. Lactoferrin attenuates intestinal barrier dysfunction and inflammation by modulating the MAPK pathway and gut microbes in mice. *J. Nutr.* 152 (11), 2451–2460. <https://doi.org/10.1093/jn/nxac200>.
- Jeon, B.T., Jeong, E.A., Shin, H.J., Lee, Y., Lee, D.H., Kim, H.J., Roh, G.S., 2012. Resveratrol attenuates obesity-associated peripheral and central inflammation and improves memory deficit in mice fed a high-fat diet. *Diabetes* 61 (6), 1444–1454. <https://doi.org/10.2337/db11-1498>.
- Karlsson, F.H., Tremaroli, V., Nookaew, I., Bergstrom, G., Behre, C.J., Fagerberg, B., Backhed, F., 2013. Gut metagenome in European women with normal, impaired and diabetic glucose control. *Nature* 498 (7452), 99–103. <https://doi.org/10.1038/nature12198>.
- Kendig, M.D., Leigh, S.J., Morris, M.J., 2021. Unravelling the impacts of western-style diets on brain, gut microbiota and cognition. *Neurosci. Biobehav. Rev.* 128, 233–243. <https://doi.org/10.1016/j.neubiorev.2021.05.031>.
- Keshavanzan, A., Green, S.J., Engen, P.A., Voigt, R.M., Naqib, A., Forsyth, C.B., Shavran, K.M., 2015. Colonic bacterial composition in Parkinson's disease. *Mov. Disord.* 30 (10), 1351–1360. <https://doi.org/10.1002/mds.26307>.
- Koliada, A., Syzenko, G., Moseiko, V., Budovska, L., Puchkov, K., Perederiy, V., Vaiserman, A., 2017. Association between body mass index and Firmicutes/Bacteroidetes ratio in an adult Ukrainian population. *BMC Microbiol.* 17 (1), 120. <https://doi.org/10.1186/s12866-017-1027-1>.
- Kuwata, H., Yamauchi, K., Teraguchi, S., Ushida, Y., Shimokawa, Y., Yoida, T., Hayasawa, H., 2001. Functional fragments of ingested lactoferrin are resistant to proteolytic degradation in the gastrointestinal tract of adult rats. *J. Nutr.* 131 (8), 2121–2127. <https://doi.org/10.1093/jn/131.8.2121>.
- Kwon, H.S., Koh, S.H., 2020. Neuroinflammation in neurodegenerative disorders: the roles of microglia and astrocytes. *Transl. Neurodegener.* 9 (1), 42. <https://doi.org/10.1186/s40035-020-00221-2>.
- Lamont, M.G., Weber, J.T., 2012. The role of calcium in synaptic plasticity and motor learning in the cerebellar cortex. *Neurosci. Biobehav. Rev.* 36 (4), 1153–1162. <https://doi.org/10.1016/j.neubiorev.2012.01.005>.
- Leigh, S.J., Morris, M.J., 2020. Diet, inflammation and the gut microbiome: mechanisms for obesity-associated cognitive impairment. *Biochim. Biophys. Acta, Mol. Basis Dis.* 1866 (6), 165767. <https://doi.org/10.1016/j.bbadis.2020.165767>.
- Ley, R.H., Turnbaugh, P.J., Klein, S., Gordon, J.I., 2006. Human gut microbes associated with obesity. *Nature* 444 (7122), 1022–1023. <https://doi.org/10.1038/4441022a>.
- Li, L., Ma, C., Hurilebag, Yuan, H., Hu, R., Wang, W., Weilisi, 2022. Effects of lactoferrin on intestinal flora of metabolic disorder mice. *BMC Microbiol.* 22 (1), 181. <https://doi.org/10.1186/s12866-022-02588-w>.
- Lituma, P.J., Woo, E., O'Hara, B.F., Castillo, P.E., Sibinga, N.E.S., Nandi, S., 2021. Altered synaptic connectivity and brain function in mice lacking microglial adapter protein Iba1. *Proc. Natl. Acad. Sci. U. S. A.* 118 (46) <https://doi.org/10.1073/pnas.2115539118>.
- Liu, S., Gao, J., Zhu, M., Liu, K., Zhang, H.L., 2020. Gut microbiota and dysbiosis in Alzheimer's disease: implications for pathogenesis and treatment. *Mol. Neurobiol.* 57 (12), 5026–5043. <https://doi.org/10.1007/s12035-020-02073-3>.
- Livak, K.J., Schmittgen, T.D., 2001. Analysis of relative gene expression data using real-time quantitative PCR and the 2<sup>-Delta Delta C(T)</sup> Method. *Methods* 25 (4), 402–408. <https://doi.org/10.1006/meth.2001.1262>.
- Livingston, G., Sommerlad, A., Orgeta, V., Bisikili, C., Costafreda, S., Huntley, J., Ames, D., Mukadam, N., Naheed, A., 2017. Dementia prevention, intervention, and care. *Lancet* 390, 2673–2734. [https://doi.org/10.1016/s0140-6736\(17\)31363-6](https://doi.org/10.1016/s0140-6736(17)31363-6), 10113.
- Lu, Y.C., Yeh, W.C., Ohashi, P.S., 2008. LPS/TLR4 signal transduction pathway. *Cytokine* 42 (2), 145–151. <https://doi.org/10.1016/j.cyto.2008.01.006>.
- Madkour, A.H., Helal, M.G., Said, E., Salem, H.A., 2022. Dose-dependent renoprotective impact of Lactoferrin against glycerol-induced rhabdomyolysis and acute kidney injury. *Life Sci.* 302, 120646. <https://doi.org/10.1016/j.ifs.2022.120646>.
- Malesza, L.J., Malesza, M., Walkowiak, J., Mussin, N., Walkowiak, D., Aringazina, R., Madry, E., 2021. High-fat, western-style diet, systemic inflammation, and gut microbiota: a narrative review. *Cells* 10 (11). <https://doi.org/10.3390/cells10113164>.
- Mohamed, W.A., Salama, R.M., Schaal, M.F., 2019. A pilot study on the effect of lactoferrin on Alzheimer's disease pathological sequelae: impact of the p-Akt/PEN pathway. *Biomed. Pharmacother.* 111, 714–723. <https://doi.org/10.1016/j.biopha.2018.12.118>.
- Nemati, M., Akseh, S., Amiri, M., Reza Nejabati, H., Jodati, A., Fathi Maroufi, N., Nouri, M., 2021. Lactoferrin suppresses LPS-induced expression of HMGB1, microRNA 155, 146, and TLR4/MyD88/NF-small ka, CyrillicB pathway in RAW264.7 cells. *Immunopharmacol. Immunotoxicol.* 43 (2), 153–159. <https://doi.org/10.1080/08923973.2021.1872616>.
- O'Brien, P.D., Hinder, L.M., Callaghan, B.C., Feldman, E.L., 2017. Neurological consequences of obesity. *Lancet Neurol.* 16 (6), 465–477. [https://doi.org/10.1016/S1474-4422\(17\)30084-4](https://doi.org/10.1016/S1474-4422(17)30084-4).
- Pan, W., Jiang, P., Zhao, J., Shi, H., Zhang, P., Yang, X., Yu, Y., 2021. beta-Glucan from *Lentinula edodes* prevents cognitive impairments in high-fat diet-induced obese mice: involvement of colon-brain axis. *J. Transl. Med.* 19 (1), 54. <https://doi.org/10.1186/s12967-021-02724-6>.
- Reseco, L., Atienza, M., Fernandez-Alvarez, M., Carro, E., Cantero, J.L., 2021. Salivary lactoferrin is associated with cortical amyloid-beta load, cortical integrity, and memory in aging. *Alzheimer's Res. Ther.* 13 (1), 150. <https://doi.org/10.1186/s13195-021-00891-8>.
- Saji, N., Niida, S., Murotani, K., Hisada, T., Tsuduki, T., Sugimoto, T., Sakurai, T., 2019. Analysis of the relationship between the gut microbiome and dementia: a cross-sectional study conducted in Japan. *Sci. Rep.* 9 (1), 1008. <https://doi.org/10.1038/s41598-018-38218-7>.
- Shaaban, A., Dhara, M., Frisch, W., Harb, A., Shaib, A.H., Becherer, U., Mohrmann, R., 2019. The SNAP-25 linker supports fusion intermediates by local lipid interactions. *Elife* 8. <https://doi.org/10.7554/eLife.41720>.
- Shen, H., Guan, Q., Zhang, X., Yuan, C., Tan, Z., Zhai, L., Han, C., 2020. New mechanism of neuroinflammation in Alzheimer's disease: the activation of NLRP3 inflammasome mediated by gut microbiota. *Prog. Neuro-Psychopharmacol. Biol. Psychiatry* 100, 109884. <https://doi.org/10.1016/j.pnpbp.2020.109884>.
- Shi, H., Wang, Q., Zheng, M., Hao, S., Lum, J.S., Chen, X., Zheng, K., 2020. Supplement of microbiota-accessible carbohydrates prevents neuroinflammation and cognitive decline by improving the gut microbiota-brain axis in diet-induced obese mice. *J. Neuroinflammation* 17 (1), 77. <https://doi.org/10.1186/s12974-020-01760-1>.
- Shukla, P.K., Delotterie, D.F., Xiao, J., Pierre, J.F., Rao, R., McDonald, M.P., Khan, M.M., 2021. Alterations in the gut-microbial-inflammasome-brain axis in a mouse model of Alzheimer's disease. *Cells* 10 (4). <https://doi.org/10.3390/cells10040779>.
- Sun, M.F., Zhu, Y.L., Zhou, Z.L., Jia, X.B., Xu, Y.D., Yang, Q., Shen, Y.Q., 2018. Neuroprotective effects of fecal microbiota transplantation on MPTP-induced Parkinson's disease mice: gut microbiota, glial reaction and TLR4/TNF-alpha signaling pathway. *Brain Behav. Immun.* 70, 48–60. <https://doi.org/10.1016/j.bbi.2018.02.005>.
- Tsatsanis, A., McCorkindale, A.N., Wong, B.X., Patrick, E., Ryan, T.M., Evans, R.W., Duce, J.A., 2021. The acute phase protein lactoferrin is a key feature of Alzheimer's disease and predictor of Abeta burden through induction of APP amyloidogenic processing. *Mol. Psychiatry* 26 (10), 5516–5531. <https://doi.org/10.1038/s41380-021-01248-1>.
- Ugalde-Trivino, L., Diaz-Guerra, M., 2021. PSD-95: an effective target for stroke therapy using neuroprotective peptides. *Int. J. Mol. Sci.* 22 (22) <https://doi.org/10.3390/ijms22212585>.
- Vorhees, C.V., Williams, M.T., 2006. Morris water maze: procedures for assessing spatial and related forms of learning and memory. *Nat. Protoc.* 1 (2), 848–858. <https://doi.org/10.1038/nprot.2006.116>.
- Xu, S.F., Zhang, Y.H., Wang, S., Pang, Z.Q., Fan, Y.G., Li, J.Y., Guo, C., 2019. Lactoferrin ameliorates dopaminergic neurodegeneration and motor deficits in MPTP-treated mice. *Redox Biol.* 21, 101090. <https://doi.org/10.1016/j.redox.2018.101090>.
- Xu, Z., Jiang, W., Huang, W., Lin, Y., Chan, F.K.L., Ng, S.C., 2022. Gut microbiota in patients with obesity and metabolic disorders - a systematic review. *Genes Nutr* 17 (1), 2. <https://doi.org/10.1186/s12263-021-00703-6>.
- Yu, S., Ren, X., Meng, F., Guo, X., Tao, J., Zhang, W., Li, L., 2022. TIM3/CEACAM1 pathway involves in myeloid-derived suppressor cells induced CD8(+) T cells exhaustion and bone marrow inflammatory microenvironment in myelodysplastic syndrome. *Immunology*. <https://doi.org/10.1111/imm.13488>.
- Zhao, M., Zhou, A., Xu, L., Zhang, X., 2014. The role of TLR4-mediated PTEN/PI3K/AKT/NF-kappaB signaling pathway in neuroinflammation in hippocampal neurons. *Neuroscience* 269, 93–101. <https://doi.org/10.1016/j.neuroscience.2014.03.039>.

- Zheng, J.P., Xie, Y.Z., Li, F., Zhou, Y., Qi, L.Q., Liu, L.B., Chen, Z., 2020. Lactoferrin improves cognitive function and attenuates brain senescence in aged mice. *J. Funct. Foods* 65. <https://doi.org/10.1016/j.jff.2019.103736>.
- Zhou, H.H., Wang, G., Luo, L., Ding, W., Xu, J.Y., Yu, Z., Wan, Z., 2021. Dietary lactoferrin has differential effects on gut microbiota in young versus middle-aged APPswe/PS1dE9 transgenic mice but no effects on cognitive function. *Food Nutr. Res.* 65 <https://doi.org/10.29219/fnr.v65.5496>.
- Zhou, X., Yuan, L., Zhao, X., Hou, C., Ma, W., Yu, H., Xiao, R., 2014. Genistein antagonizes inflammatory damage induced by beta-amyloid peptide in microglia through TLR4 and NF-kappaB. *Nutrition* 30 (1), 90–95. <https://doi.org/10.1016/j.nut.2013.06.006>.